CardioVascular and Interventional Radiology

LABORATORY INVESTIGATIONS

MR-Guided Percutaneous Angioplasty: Assessment of Tracking Safety, Catheter Handling and Functionality

Simon Wildermuth,[1] Charles L. Dumoulin,[2] Thomas Pfammatter,[1] Stephan E. Maier,[3] Eugen Hofmann,[4] Jörg F. Debatin[1]

[1]Institute of Diagnostic Radiology, University Hospital Zürich, CH-8091 Zurich, Switzerland
[2]GE Corporate Research and Development Center, P.O. Box 8, 1 River Road, Schenectady, NY 12301, USA
[3]Department of Radiology, Brigham and Women's Hospital, Harvard Medical School, 75 Francis Street, Boston, MA 02115, USA
[4]Schneider (Europe), Ackerstrasse 6, CH-8180 Bülach, Switzerland

Abstract

Purpose: Magnetic resonance (MR)-guided percutaneous vascular interventions have evolved to a practical possibility with the advent of open-configuration MR systems and real-time tracking techniques. The purpose of this study was to assess an MR-tracking percutaneous transluminal angioplasty (PTA) catheter with regard to its safety profile and functionality.
Methods: Real-time, biplanar tracking of the PTA catheter was made possible by incorporating a small radiofrequency (RF) coil in the catheter tip and connecting it to a coaxial cable embedded in the catheter wall. To evaluate potentially hazardous thermal effects due to the incorporation of the coil, temperature measurements were performed within and around the coil under various scanning and tracking conditions at 1.5 Tesla (T). Catheter force transmission and balloon-burst pressure of the MR-tracking PTA catheter were compared with those of a standard PTA catheter. The dilatative capability of the angioplasty balloon was assessed in vitro as well as in vivo, in an isolated femoral artery segment in a swine.
Results: The degree of heating at the RF coil was directly proportional to the power of the RF pulses. Heating was negligible with MR tracking, conventional spin-echo and low-flip gradient-echo sequences. Sequences with higher duty cycles, such as fast spin echo, produced harmful heating effects. Force transmission of the MR-tracking PTA catheter was slightly inferior to that of the standard PTA catheter, while balloon-burst pressures were similar to those of conventional catheters. The MR-tracking PTA catheter functioned well both in vitro and in vivo.

Conclusion: The in vivo use of an MR-tracking PTA catheter is safe under most scanning conditions.

Key words: Interventional MRI—MR angiography—Percutaneous transluminal angioplasty—MRI, bioeffects

Fundamental to the success and safety of percutaneous transluminal angioplasty (PTA) is the visualization of the catheter tip relative to the area of treatment. To date this has been achieved with X-ray fluoroscopy. Exposure to ionizing radiation, limited contrast, adverse reactions following the application of iodinated agents, and the inability to image in cross-section have motivated the exploration of alternate imaging strategies.

Magnetic resonance imaging (MRI) causes no radiation exposure, is capable of combining high temporal and spatial resolution [1], and provides images in any desired plane. The motion sensitivity inherent in MRI obviates the need for contrast agents in order to visualize vascular structures. Its soft tissue contrast is vastly superior to that of fluoroscopy, permitting the concurrent evaluation of tissues surrounding the vessel of interest. Furthermore, quantitative velocity and flow-volume characterization can be integrated in the same noninvasive vascular evaluation [2]. With the advent of open MR systems providing direct access to patients, the concept of MR-based PTA catheter guidance and control has evolved from a hypothetical concept to a practical possibility [3].

Dumoulin et al. [4] have developed a technique for active MR tracking of devices under near real-time conditions. As first suggested by Ackerman et al. [5], a small receive-only coil is incorporated into the tip of the device. Following non-selective radiofrequency (RF) excitation of a volume

Correspondence to: J. F. Debatin, M.D.
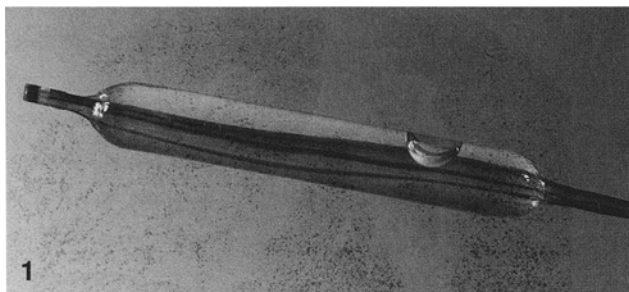
Fig. 1. Proximal portion of the 5.3 Fr MR-tracking PTA catheter contains the cylindrical balloon, which extends over 40 mm and can be inflated to a diameter of 6 mm. The coaxial cable, embedded in the catheter wall, is also seen. The coil is positioned at the catheter's tip, 10 mm distal to the balloon.
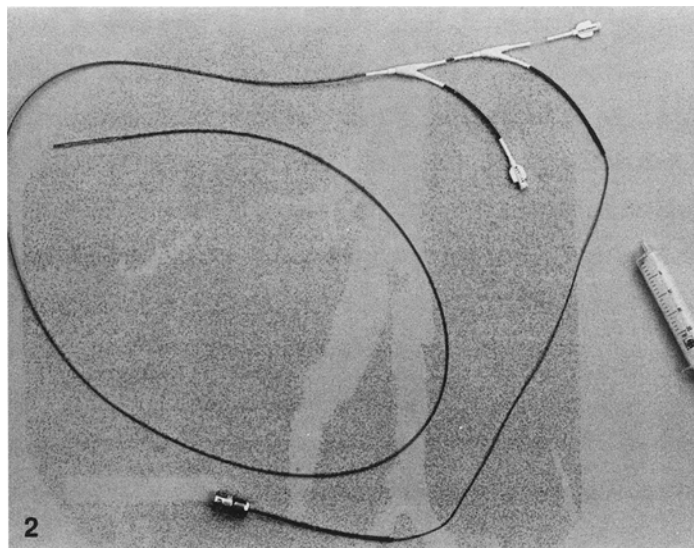
Fig. 2. Overview of the MR-tracking PTA catheter with a deflated balloon. Next to two luer locks the coaxial plug from which the signal is fed into the scanner is visible.

defined by the dimensions of the field of view, a gradient-recalled echo (GRE) is generated by the coil situated in the tip of the catheter (Fig. 1). Following Fourier transformation, a signal peak is obtained, the frequency of which corresponds to the position of the coil on a particular axis. A Hadamard multiplexed pulse sequence is used in which positional information from all three axes is multiplexed and acquired simultaneously [6]. Thus, the three-dimensional position of the coil is encoded with four excitations, and the coil's position can be computed up to 20 times per second. The catheter tip's position is displayed by graphic overlay as a cursor on any previously acquired MR image. This composite image is projected onto a screen visible to the operator in the scan room and video-taped for archiving purposes. Simultaneous tracking in two planes is possible with this technique [7].

The localizing accuracy of this real-time tracking technique has been documented both in vitro and in vivo, using straight non-therapeutic catheters [8]. In the current study active tracking was implemented into a complex dual-lumen PTA catheter, whereby a coil, connected to a fully insulated coaxial wire, was built into the tip of a catheter distal to the angioplasty balloon.

The introduction of conducting materials into an MRI system can potentially lead to thermal, electrical, and other hazardous effects. Furthermore, incorporation of a coil and coaxial cable into an already complex PTA catheter design affects its handling characteristics. The purpose of this study was to address these safety concerns with regard to intravascular coil heating as well as PTA catheter handling and balloon function, in preparation for a first human percutaneous angioplasty.

Materials and Methods

Design of the MR-Tracking PTA Catheter

Special MR-tracking PTA catheters were constructed by Schneider Europe (Bülach, Switzerland). At its tip, the catheter is equipped with a copper RF coil consisting of 16 loops with an outer diameter of 1.1 mm (Fig. 1). The coils are incorporated into the catheter material itself and are connected to a plug at the base of the catheter via a fully insulated coaxial cable with a diameter of 0.38 mm, embedded in the catheter wall (Fig. 2). The catheter is 120 cm long and contains a standard 0.035-inch lumen for placement of a guidewire. It is made of polyamide (PM 200, Schneider), a highly flexible material providing optimum force transmission and covered with Softglide coating. The material is approved for human use and is already found in commercially available catheters. Design of the MR-tracking PTA catheter, 5.3 Fr in diameter, is based on the SMASH model (Schneider). The cylindrical balloon portion extends over 40 mm, from 10 mm to 50 mm proximal to the coil at the catheter's tip (Fig. 1). The balloon is made of a special polyamide (PM 300, Schneider). The inflated balloon diameter is 6 mm, and has a recommended pressure range of 5–10 atm (burst pressure 14–18 atm).

Evaluation of Catheter Properties

Catheter force transmission (trackability) was assessed for the 5.3 Fr coil-tipped PTA catheter in comparison with a standard 5 Fr SMASH balloon catheter (Schneider). The catheters were placed in a guidance system (inside diameter 2.5 mm) with several preformed bends. Force transmission, expressed in newtons (N), was monitored and plotted continuously over distance as the PTA catheters, stabilized with Teflon-coated 0.035-inch guidewires, were mechanically advanced for 140 mm around a 90° bend with a 12-mm radius within the guidance system. For both catheters, the areas under the

force transmission curves were determined. Subsequently, balloon-burst pressures were determined for the modified 5.3 Fr MR-tracking PTA catheter and compared with those of a standard 5 Fr SMASH PTA model.

Heating of MR-Tracking PTA Catheters

Initial experiments were performed on a 1.5 MR system (SIGNA, General Electric, Milwaukee, WI, USA), using the body coil for RF excitation. The MR-tracking PTA catheter (equipped with an integral 16-turn pickup coil at its tip) was evaluated in a phantom consisting of a foam box with 2-inch-thick walls, containing a cylindrical jar. To prevent heat dissipation, the jar was filled with a gel plug prepared from agar and normal saline. The catheter and fiberoptic probe were inserted through small holes in the lid of the box. Temperature was measured simultaneously at different locations both around and directly inside the coil using the fiberoptic temperature probe (Luxtron, Santa Clara, CA, USA). Temperature data were acquired 4 times per second, and averaged every second. The average data were sent via high-speed data link to a Sparc 10 (Sun Microsystems, Palo Alto, CA, USA) workstation, where they were stored.

For each experiment, the temperature was monitored over 15 min with the probe located inside the coil at the tip of the catheter, which was aligned orthogonally to the body coil (along the x-axis). Scanning was commenced at 5:00 min. Using a transmitter gain setting of 72 centibels (determined by auto-prescan procedure), the temperature effects of five different sequences were assessed:

Fast spin echo (FSE) (TR/TE 2000/16, 80 msec; 4 excitations, scan time 4:20 min)
Conventional spin echo (SE) (TR/TE 800/16 msec; 1 excitation, scan time 3:31 min)
Gradient-recalled echo (GRE) (TR/TE 8/4 msec; 150 excitations, flip angle 45°, scan time 5 min)
Gradient-recalled echo (GRE) (TR/TE 8/4 msec; 150 excitations, flip angle 90°, scan time 5 min)
MR-tracking (TR/TE 13.9/4 msec; flip angle 90°; 18 tracking updates/sec, scan time 5 min)

Temperature measurements during FSE scanning were repeated with and without gradient and RF power. The effect of catheter orientation in the magnet was evaluated by performing the FSE experiment twice: once with the catheter placed along the x-axis and a second time along the z-axis. To determine the localization of maximal heating, temperature changes during FSE scanning were determined inside the coil, immediately adjacent to it, and at 0.5, 1, 2, 3, 4, 5, 10, 15, 20, 25, and 30 cm from the tip.

Assessment of MR-Tracking PTA Catheter Function

The function of the MR-tracking PTA catheter was assessed in vitro using a flow phantom, as well as in vivo in a fully anesthetized 45-kg swine. Both experiments were performed in an "open configuration" interventional 0.5 T MR system (SIGNA MRT, General Electric).

A harvested segment (12 cm) of human common femoral artery was connected to 9-mm Tygon tubing at both ends and placed in a gel-filled Plexiglas container. The proximal end of the tubing was connected to a roller flow pump, adjusted to deliver 300 ml/min. The distal end of the tubing merged into a vented reservoir from which the pump was supplied. A 2-cm-long, high-grade stenosis (80% diameter reduction) was created in the center of the harvested vessel segment by placing soft modeling dough around it. A time-of-flight (TOF) "road map" data set [TR/TE 33/8 msec, flip angle 30°, 5-mm sections, FOV 40 cm, 256 × 192 matrix, first-order gradient moment nulling, 1 NEX (number of excitations)] was acquired, depicting the vessel and the stenosis. Subsequently the PTA catheter was introduced into the phantom through a luer lock proximal to the harvested vessel segment. The stenosis was crossed under MR-tracking guidance (TR/TE/flip 13.9 msec/4 msec/60°) rendering 18 updates/sec. Upon withdrawing the catheter, the tip was placed 2 cm distal to the stenosis to assure proper coverage of the stenosis by the balloon. The balloon was inflated to 4 atm. The MR angiographic TOF road map was repeated following withdrawal of the PTA catheter.

The in vivo animal experiment had been approved by the appropriate governmental regulatory committees. As premedication 2.0 ml azaperone and 0.7 ml atropine were administered. The swine was ventilated at all times with an anesthetic containing halothane and oxygen. The carotid arteries were surgically accessed by arteriotomy. Under fluoroscopic guidance a 6 Fr introducer sheath was passed over a guidewire into the carotid arteries and secured by suture. Through the indwelling introducer, the MR-tracking PTA catheter was advanced into the descending aorta. To enhance maneuverability, the catheter tip had been slightly curved manually over hot steam prior to insertion. The animal was subsequently transferred to the interventional MRI system where coronal MR angiographic TOF road maps of the abdominal aorta and its branches were acquired. Based on these images, the PTA catheter was manipulated under active MR-tracking guidance without the presence of a guidewire, using parameters identical to those employed in the phantom experiment, into the right renal artery. The balloon was inflated with undiluted gadolinium-DTPA (Magnevist, Schering, Berlin, Germany) to 2 atm. Coronal TOF images confirmed occlusion of the renal artery with the inflated balloon.

Results

Properties of the MR-Tracking PTA Catheter

The coil-tipped 5.3 Fr MR-tracking PTA catheter was characterized by 18% poorer force transmission compared with the conventional 5.0 Fr SMASH PTA catheter as determined by the difference of the areas under the force transmission curves (Fig. 3). Burst pressures of the two balloons were almost identical: the burst pressure of the balloon mounted on the conventional catheter was recorded at 16.9 atm, while that of the balloon integrated in the MR-tracking PTA catheter was 17.2 atm.

Heating of the MR-Tracking PTA Catheter

All the forms of MRI scanning evaluated resulted in some heating as determined by the temperature probe located inside the coil. There were considerable differences, however, in the degree of heating associated with the various
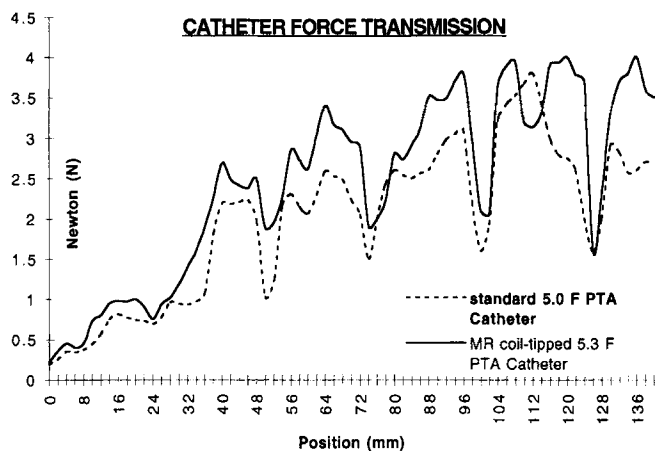
Fig. 3. Assessment of catheter force transmission (trackability), expressed in newtons (N), of a normal 5.0 Fr SMASH PTA catheter and a coil-tipped 5.3 Fr MR-tracking PTA catheter over a 140-mm distance, negotiating a preformed 90° turn (radius 12 mm). The area under the MR catheter curve exceeds that of the conventional catheter by 18%.

Fig. 4. Temperature gradient from the tracking coil itself, using a fast spin echo (FSE) sequence. Heating is concentrated near the tip of the catheter and falls off dramatically as the distance from the coil is increased.

Table 1. Heating effects of various pulse sequences

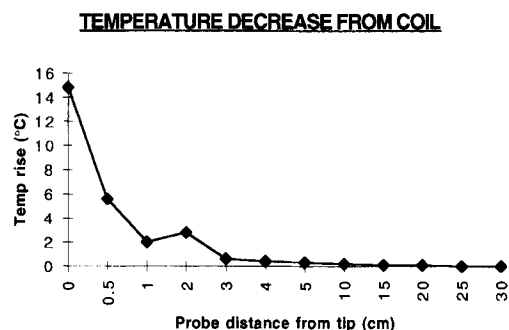| Type of sequence	Flip angle (deg)	Scan time (min)	Temperature rise (°C)[a]
Fast spin echo		4:20	19.9 ± 0.76
Conventional spin echo		3:31	1.7 ± 0.12
Gradient-recalled echo	45°	5:00	4.8 ± 0.19
Gradient-recalled echo	90°	5:00	17.7 ± 0.53
MR tracking	90°	5:00	1.7 ± 0.14

[a] Mean ± SD

sequences. The greatest temperature increase was recorded with FSE scanning (19.9°C); the smallest with conventional SE (0.6°C) (Table 1). The flip angle used in the GRE sequence had a major impact: a flip angle of 45° resulted in a temperature rise of 4.8°C, whereas a 90° flip angle induced an increase of 17.7°C. The MR-tracking sequence, employing a flip angle of 90° and permitting 18 updates/sec was associated with only a small temperature rise of 1.7°C.

While scanning with and without gradient power yielded identical temperature changes in the center of the coil, no heating at all was observed when the RF power was turned off.

The orientation of the catheter within the magnet had a considerable impact on the degree of heating measured within the coil. Maximal heating was caused by placing the catheter orthogonal (along the x-axis) to the axis of the body coil. Changing the catheter orientation to parallel the axis of the body coil (along the z-axis) significantly reduced the heating from 19.9°C to a minimum of only 1.4°C.

Heating was concentrated near the tip of the catheter and was maximal inside the coil itself (19.9°C). There is a steep

temperature gradient as the distance from the catheter is increased (Fig. 4). Immediately adjacent to the coil a maximal temperature increase of 14.8°C was recorded, while the temperature 10 mm from the tip of the catheter increased by only 2.0°C.

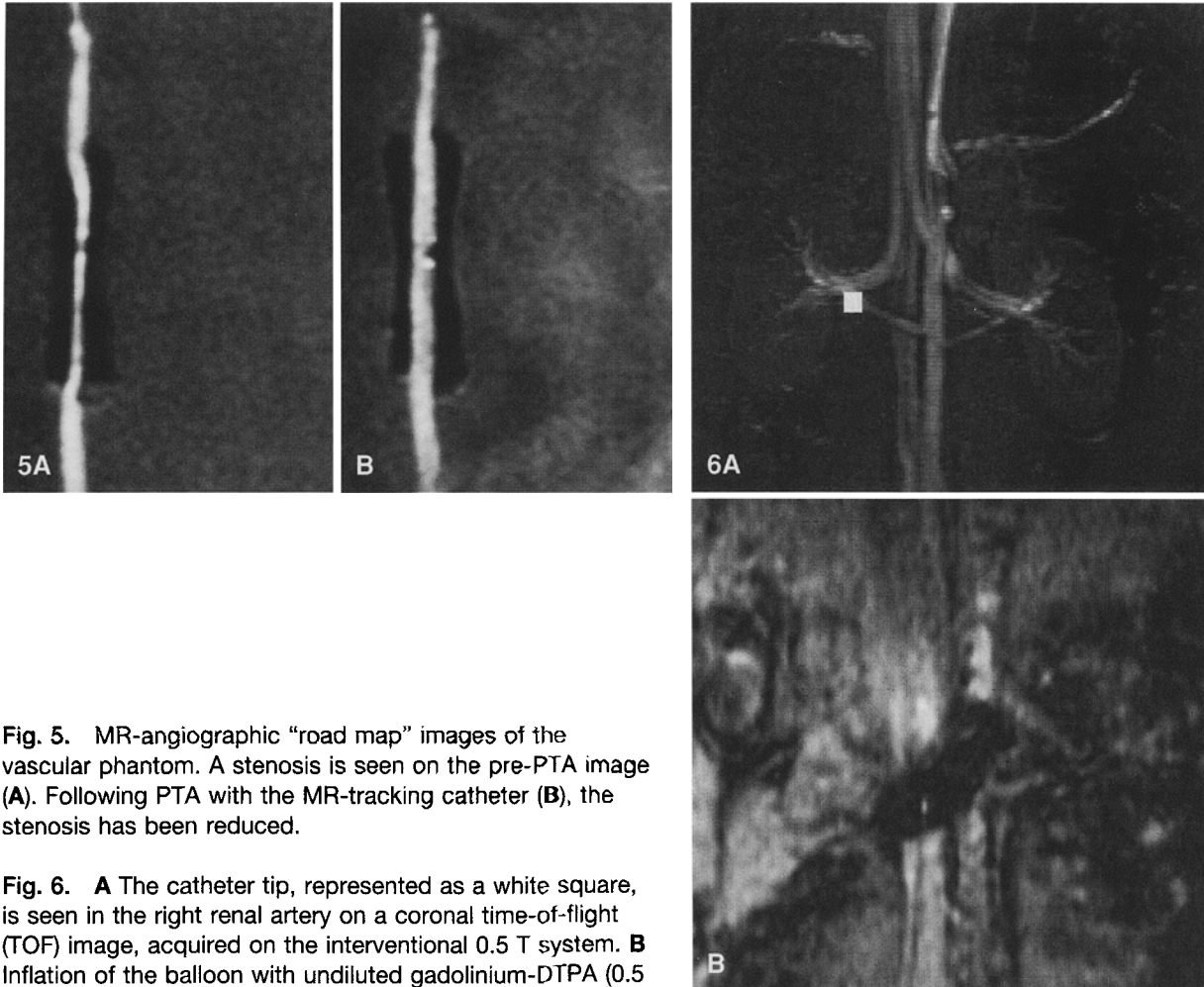## Function of the MR-Tracking PTA Catheter

The MR-tracking PTA catheter functioned well both in vitro and in vivo. Using TOF MR-angiographic road maps (Fig. 5A), the catheter was manipulated to its desired position in both instances. Under MR-tracking guidance the stenosis was negotiated with ease in vitro, and in vivo the MR-tracking PTA catheter was successfully maneuvered into the right renal artery even under pulsatile flow conditions.

Based on the TOF road map of the flow phantom, the tip of the MR-tracking PTA catheter was correctly positioned, assuring complete coverage of the artificial stenosis by the balloon. Inflating the balloon reduced the stenosis as documented by the post-dilatation MR angiogram (Fig. 5B). Tracking remained possible with the balloon inflated. Similarly, tracking was not affected when a 0.035-inch nitinol guidewire (RoadRunner, Cook Medical Systems, Bjaeverskov, Denmark) was introduced through the catheter.

Inflation of the balloon with undiluted gadolinium-DTPA, situated within the right renal artery, rendered the outline of the inflated balloon dark (Fig. 6A). On subsequently acquired TOF road map images this dark signal contrasted well with the high signal from surrounding flowing spins. TOF road maps confirmed occlusion of the right renal artery when the balloon, situated in the renal artery, was inflated (Fig. 6B).

Discussion

This study describes the potential and limitations of various hardware and software components that are part of an evolving concept using MRI for guidance and monitoring of PTA in peripheral arteries. In vitro and in vivo analysis of the various components demonstrated that most of the require-

Fig. 5. MR-angiographic "road map" images of the vascular phantom. A stenosis is seen on the pre-PTA image (**A**). Following PTA with the MR-tracking catheter (**B**), the stenosis has been reduced.

Fig. 6. **A** The catheter tip, represented as a white square, is seen in the right renal artery on a coronal time-of-flight (TOF) image, acquired on the interventional 0.5 T system. **B** Inflation of the balloon with undiluted gadolinium-DTPA (0.5 M) renders the angioplasty balloon black.

ments essential to the success of PTA can be met using the outlined concept. These include: real-time visualization of the PTA catheter tip and its relation to the vascular stenosis, biocompatibility of the catheter materials and safety of the PTA catheter within vessels, appropriate handling characteristics of the catheter permitting flexible intravascular use, and proper functioning and visualization of the inflated PTA balloon inside the vessel.

There are two fundamental approaches to device localization with MRI: electrically passive techniques based on visualization of susceptibility-induced signal voids caused by the instrument itself [9], and electrically active techniques. The passive approach is already being used for biopsy needle guidance [10]. Its dependence on field strength, device orientation, and particular pulse sequence parameters make passive visualization volatile and not sufficiently reliable to guide complex intravascular interventions [9]. As has been previously shown, active visualization of instruments with MR tracking is highly accurate and reliable [7, 8]. Furthermore, MR tracking is virtually independent of device orientation and provides maximal flexibility with regard to the characteristics of the underlying MR image on which the instrument-tracking is based. A position update 18

times per second with a display delay of under 10 msec ensures real-time tracking of the instrument. With biplanar implementation of display, it is possible to track any instrument in real time simultaneously in any two planes [8, 11].

Active MR-tracking does, however, require the integration of a coil-antenna connected to a transmitting cable [4] into the instrument itself. The accuracy and robustness of MR-tracking positioning is ultimately determined by the signal-to-noise ratio of the detected MR signal. Accuracy and tracking reliability can be enhanced by maximizing the signal-to-noise ratio. Based on in vitro data, which had documented a linear relationship between the height of the MR tracking signal peak and the number of coil turns [8], the miniaturized receiver coil in the tip of the catheter was constructed with 16 turns. To eliminate background signal that might impede robust tracking [8], a fully shielded coaxial cable was used to transmit the signal from the coil to the catheter base.

The MR-tracking PTA catheters were designed to emulate the characteristics of catheters currently available for fluoroscopically guided PTA. Although both the copper coil and the coaxial cable are made of biocompatible materials,

they were fully covered by polyamide, a biocompatible catheter material, as an added safety feature. The 1.1-mm diameter of the 16-turn coil was sufficiently small to permit implementation in the catheter tip itself; integration of the coaxial cable with a diameter of 0.38 mm into the standard 5.0 Fr PTA catheter, on the other hand, required a slight increase in catheter size from 5.0 to 5.3 Fr.

Despite this increase in the catheter's diameter and the addition of the coil and the coaxial cable, in vitro evaluations revealed the force transmission of the coil-tipped PTA catheter to be only 18% poorer compared with the conventional 5.0 Fr system. This effect could be further mitigated by use of thinner coaxial cables and tighter coil windings. Even the current design was sufficiently flexible however, to permit maneuvering of the MR-tracking PTA catheter both in vitro and in vivo. The ability to negotiate even the very steep origins of the renal arteries found normally in pigs (Fig. 6A) must be considered highly encouraging. Clearly further optimization of catheter design is warranted, however.

The introduction of conducting materials into the MRI system does lead to thermal effects, as documented by the in vitro experiments at 1.5 T. In accordance with other reports [12], all heating observed in and near devices appeared to be caused by the RF pulses from the MRI system transmitter (body coil). Thus no heating at all was observed when the RF power was turned off. Magnetic field gradient activity, on the other hand, had no effect on the extent of heating.

The degree of heating at the RF coil was directly proportional to the power of the RF pulses. This is reflected by the temperature data collected under various scanning conditions. Doubling the flip angle of the GRE sequence resulted in an almost four-fold increase in temperature rise. Similarly, the FSE sequence with a long RF duty cycle was characterized by far greater heating than the conventional SE scan with a far shorter duty cycle.

These experimental measurements represent "worst case" heating conditions. Temperatures were measured over a long scanning interval during which a temperature equilibrium plateau could be established. Cooling effects from flowing blood were disregarded. Most significantly, the catheter was oriented orthogonal to the transmitting source, resulting in maximal heating. Furthermore the temperature probe was situated within the coil itself, where the heat effect was most concentrated. Even though heat dissipation was limited by use of an agar gel phantom, a steep temperature gradient was found as the temperature probe was moved away from the coil. Finally, the experiments were performed at a field strength of 1.5 T. Since heating is proportional to the RF power, heating at a field strength of 0.5 T can be expected to be $(0.5/1.5)^2$, or one-ninth that observed at 1.5 T.

To avoid any potential damage to tissues or blood, the maximal temperature rise should not exceed 4°C [13]. At a field strength of 0.5 T none of the evaluated scanning conditions would have exceeded this safety heating tolerance. At 1.5 T, on the other hand, sequences with higher RF duty cycles did produce harmful heating effects. Thus heating

from FSE scanning is unacceptable. Similarly, the flip angle of GRE sequences should be limited to 30°. Conventional SE imaging and MR-tracking at a maximal refresher rate of 18/sec, on the other hand, are without harm even at 1.5 T.

Tracking of the PTA catheter was based on MR angiographic TOF road map images. The catheter's tip was consistently visualized under both in vitro and pulsatile in vivo conditions. Guided by MR tracking, the balloon of the PTA catheter was correctly positioned in a predefined vascular segment allowing for the successful reduction of the artificial stenosis in the flow phantom. Similarly, the PTA catheter was placed into the right renal artery of the swine in a manner permitting easy occlusion of the vessel. The contours of the inflated balloon were made visible by filling it with undiluted gadolinium-DTPA. This paramagnetic contrast material has a viscosity similar to that of conventional iodinated agents.

The balloon characteristics of the MR-tracking PTA catheter are similar to those of commercially available PTA catheters, as reflected by the comparable burst pressure determinations. The dilatative ability of an MR-tracking PTA catheter was demonstrated in the segment of harvested human femoral artery (Fig. 5). Clearly though, the ability to negotiate and treat high-grade atherosclerotic lesions still needs to be demonstrated in vivo prior to clinical implementation of this technique.

In its current implementation, the technique is highly sensitive to motion. Once motion does occur, the TOF road map images on which the MR tracking is based need to be updated, or at least modified. Such updates are time-consuming with conventional techniques. While the implementation of ultrafast imaging [14, 15] will reduce these update times, it will also exacerbate heating effects, limiting its use to a field strength of 0.5 T. Other solutions, also applicable to 1.5 T systems, include the use of "navigator sequences" [16, 17], capable of compensating for cyclical motion such as respiration. By determining the position of the diaphragm every 100 msec, the positional MR-tracking information could be corrected accordingly. Until the implementation of these techniques in an interventional MR-angiography environment, however, the motion-induced need for time-consuming road map updates will remain a significant hurdle.

Another difficult issue remains that of an MR-compatible guidewire. To prevent vessel injury a guidewire should be used for all intravascular procedures. For effective manipulation, a guidewire needs to be visualized along its length, not just at a single point. Passively visible materials have been investigated [9] with limited success. Visualization by means of positive contrast would be preferable. Such an approach was recently proposed, whereby a simple, electrically coupled stub antenna is used for signal reception. The combination of such guidewires with MR tracking of catheters has yielded encouraging preliminary in vitro results [18].

The concept of MR-guided PTA might be further enhanced by the application of intravascular receiver coils for high-resolution imaging of vessel walls [19–21]. The coil

built into the catheter tip could be used for imaging in addition to tracking, allowing direct characterization of vascular lesions. In conjunction with conventional MR angiography and noninvasive flow quantitation, these possibilities constitute a fascinating, integrative MR-based approach to percutaneous transluminal angioplasty.

References

1. Edelmann RR (1993) MR angiography: Present and future. AJR 161: 1–11
2. Pelc NJ, Herfkens RJ, Shimakawa A, Enzmann DR (1991) Phase contrast cine magnetic resonance imaging. Magn Reson Q 7:229–254
3. Schenck JF, Jolesz FA, Roemer PB, Cline HE, Lorensen WE, Kikinis R, Silverman SG, Hardy CJ, Barber WD, Laskaris ET (1995) Superconducting open-configuration MR imaging system for image-guided therapy. Radiology 195:805–814
4. Dumoulin CL, Souza SP, Darrow RD (1993) Real-time position monitoring of invasive devices using magnetic resonance. Magn Reson Med 29:411–415
5. Ackerman JL, Offut MC, Buxton RB, Brady TJ (1986) Rapid 3D tracking of small RF coils. In: Book of Abstracts: Society of Magnetic Resonance in Medicine. Society of Magnetic Resonance in Medicine, Berkeley, CA, p 1131
6. Dumoulin CL, Souza SP, Darrow RD, Pelc NJ, Adams WJ, Ash SA (1991) Simultaneous acquisition of phase contrast angiograms and stationary tissue images with Hadamard encoding of flow-induced phase shifts. J Magn Reson Imaging 1:399–404
7. Leung DA, Debatin JF, Wildermuth S, Heske N, Dumoulin CL, Darrow RD, Hauser M, Davis CP, von Schulthess GK (1995) Real-time biplanar needle tracking for interventional MR imaging procedures. Radiology 197:485–488
8. Leung DA, Debatin JF, Wildermuth S, McKinnon GC, Holtz D, Dumoulin CL, Darrow RD, Hofmann E, von Schulthess GK (1995) Intravascular MR tracking catheter: Preliminary experimental evaluation. AJR 164:1265–1270
9. Koechli VD, McKinnon GC, Hofmann E, von Schulthess GK (1994) Vascular interventions guided by ultrafast MR imaging: Evaluation of different materials. Magn Reson Med 31:309–314
10. Lufkin RB, Teresi L, Hanafee WN (1987) New needle for MR-guided aspiration cytology of the head and neck. AJR 149:380–382
11. Wildermuth S, Debatin JF, Leung DA, Hofmann E, Dumoulin CL, Darrow RD, Schöpke WD, Uhlschmid G, McKinnon GC, von Schulthess GK (1995) MR-guided percutaneous intravascular interventions: In vivo assessment of potential applications. In: Book of Abstracts: Society of Magnetic Resonance in Medicine. Society of Magnetic Resonance in Medicine, Berkeley, CA, p 428
12. Buchli R, Boesiger P, Meier D (1988) Heating effects of metallic implants by MRI examinations. Magn Reson Med 7:255–261
13. Knapp WH, Debatin JF, Helus F, Sinn HJ, Ostertag H (1989) Increased thermal response to ultrasound in the Walker carcinosarcoma treated with vasoactive drugs. Cancer Res 49:1768–1772
14. Mansfield P (1977) Multiplanar image formation using NMR spin-echoes. J Phys C 10:L55–L58
15. Wetter DR, McKinnon GC, Debatin JF, von Schulthess GK (1995) Cardiac echo-planar MR imaging: Comparison of single- and multiple-shot techniques. Radiology 194:765–770
16. Pelc NJ, Bernstein MA, Shimakawa A, Glover GH (1991) Encoding strategies for three-direction phase-contrast MR imaging of flow. J Magn Reson Imaging 1:405–413
17. Hausmann R, Lewin JS, Laub G (1991) Phase-contrast MR angiography with reduced acquisition time: New concepts in sequence design. J Magn Reson Imaging 1:415–422
18. Ladd ME, Erhart P, Debatin JF, Hofmann E, Boesiger P, von Schulthess GK, McKinnon GC (1997) Guidewire antennas for MR fluoroscopy. Magn Reson Med 37:891–897
19. Hurst GC, Hua J, Duerk JL, Cohen AM (1992) Intravascular (catheter) NMR receiver probe: Preliminary design analysis and application to canine iliofemoral imaging. Magn Reson Med 24:343–357
20. Kandarpa K, Jakab P, Patz S, Schoen FJ, Jolesz FA (1993) Prototype miniature endoluminal MR imaging catheter. J Vasc Interv Radiol 4:419–427
21. Zimmermann GG, Erhart P, Schneider J, von Schulthess GK, Schmidt M, Debatin JF (1997) Intravascular MR imaging of atherosclerotic plaque: Ex vivo analysis of human femoral arteries with histologic correlation. Radiology 204:769–774